STEM CELLS AND DEVELOPMENT
Volume 00, Number 00, 2018

DOI: 10.1089/scd.2018.0010

Transplanted Human Pluripotent Stem Cell-Derived Mesenchymal Stem Cells Support Liver Regeneration in Gunn Rats

Lucas-Sebastian Spitzhorn,[1,*] Claus Kordes,[2,*] Matthias Megges,[1] Iris Sawitza,[2] Silke Götze,[2] Doreen Reichert,[2] Peggy Schulze-Matz,[1] Nina Graffmann,[1] Martina Bohndorf,[1] Wasco Wruck,[1] Jan Philipp Köhler,[2] Diran Herebian,[3] Ertan Mayatepek,[3] Richard O.C. Oreffo,[4] Dieter Häussinger,[2,†] and James Adjaye[1,†]

Gunn rats bear a mutation within the uridine diphosphate glucuronosyltransferase-1a1 (*Ugt1a1*) gene resulting in high serum bilirubin levels as seen in Crigler-Najjar syndrome. In this study, the Gunn rat was used as an animal model for heritable liver dysfunction. Induced mesenchymal stem cells (iMSCs) derived from embryonic stem cells (H1) and induced pluripotent stem cells were transplanted into Gunn rats after partial hepatectomy. The iMSCs engrafted and survived in the liver for up to 2 months. The transplanted iMSCs differentiated into functional hepatocytes as evidenced by partially suppressed hyperbilirubinemia and expression of multiple human-specific hepatocyte markers such as albumin, hepatocyte nuclear factor 4α, *UGT1A1*, cytokeratin 18, bile salt export pump, multidrug resistance protein 2, Na/taurocholate-cotransporting polypeptide, and α-fetoprotein. These findings imply that transplanted human iMSCs can contribute to liver regeneration in vivo and thus represent a promising tool for the treatment of inherited liver diseases.

Keywords: ESC, iPSC, iMSC, stem cell transplantation, liver regeneration, fetal MSC

Introduction

The Crigler-Najjar syndrome was first reported in 1952 as an inherited disorder causing jaundice and kernicterus in newborns [1]. To date, phototherapy remains the standard treatment option to prevent the neurotoxic effects of increased bilirubin levels [2]. Phototherapy significantly influences patient's quality of life and can cause DNA damage [3]. Other treatment options such as liver transplantation, liver-directed gene therapy [4], and hepatocyte transplantation [5] require matching donors or involve suppression of the recipient's immune system. Thus, there is an urgent unmet need for alternative treatment options for Crigler-Najjar syndrome. The Gunn rat serves as an animal model to study Crigler-Najjar syndrome 1. Gunn rats have a mutation in the uridine diphosphate glucuronosyltransferase-1a1 (*Ugt1a1*) gene associated with decreased glucuronidation and excretion of bilirubin leading to hyperbilirubinemia [6].

Mesenchymal stem cells (MSCs) are currently under investigation for the treatment of liver diseases. The main reasons for the application of MSCs reside in their ability to home-in into sites of injury and modulate the immune system by secretion of supportive factors that make them widely used for treating graft-versus-host disease. The potential of MSCs to develop into bone, cartilage, and fat cells and the presence of the cell surface markers CD73, CD90, CD105, CD146, and platelet-derived growth factor receptor β (PDGFRβ) are well established and often used as criteria for characterizing them [7,8]. In addition, MSCs are reported to be able to differentiate into other organ-specific cells such as functional liver cells in vitro and in vivo [9,10]. An increasing number of studies have shown that MSCs can contribute to liver regeneration either directly or indirectly through the secretion of beneficial trophic factors [11]. However, some studies have reported that MSCs can also exert adverse effects, such as contributing to fibrosis in several organs [12,13].

Most researchers typically use MSCs from distinct sources such as bone marrow, cord blood, adipose tissue, and amniotic fluid [14]. The use of these MSCs is wrought with

[1]Institute for Stem Cell Research and Regenerative Medicine, [2]Clinic of Gastroenterology, Hepatology and Infectious Diseases, and [3]Department of General Pediatrics, Neonatolgy and Pediatric Cardiology, Heinrich Heine University, Düsseldorf, Germany.
[4]Centre for Human Development, Stem Cells and Regeneration, Faculty of Medicine, University of Southampton, Southampton, United Kingdom.
*These two authors contributed equally to this work.
†Shared senior authorship.

several limitations such as limited expansion. In light of this, the concept of generating MSCs from induced pluripotent stem cells (iPSCs) is of great interest for stem cell-based therapies given their potential immunosuppressive and regenerative properties, which are maintained in pluripotent stem cell-derived MSCs, termed induced MSCs (iMSCs). It has been shown that iMSCs have the typical mesenchymal morphology, in vitro differentiation potential, cell surface marker expression, and similar transcriptomes to bone marrow-derived MSCs [15]. Interestingly, iMSCs seem to be more potent than their native counterpart [16,17]. Furthermore, the regenerative potential of iMSCs has been demonstrated in animal models of diseases such as multiple sclerosis, limb ischemia, autoimmunity and hypoxic ischemia [16–20].

It has been shown that bone marrow-derived MSCs and hepatocyte-like cells from human iPSCs can improve the disease phenotype in Gunn rats [21,22]. In this study, we addressed the question whether iMSCs from human embryonic stem cells (ESCs) and human iPSCs are an alternative cell source for the regeneration of hereditable liver defects in vivo. The iMSCs derived from both sources were transplanted through the spleen into Gunn rats with an injured liver (partial hepatectomy). By adopting this approach, we could show the ability of the iMSCs to (1) home into the injured liver, (2) bypass rejection by the host immune system, and (3) acquire hepatocyte expression and function, thereby supporting regeneration of the injured liver.

Materials and Methods

Generation of iMSCs

Fetal MSCs (fMSCs, 55 days postconception) [23,24] were obtained from human femur following informed written patient consent and approval (Southampton and South West Hampshire Local Research Ethics Committee, LREC 296100). The experimental use of human fMSCs was approved by the ethics commission of the Heinrich Heine University, Düsseldorf. The fMSCs were cultured in α-MEM (minimum essential medium Eagle–alpha modified; Sigma-Aldrich, Taufkirchen, Germany) supplemented with 10% fetal bovine serum (FBS), 1% GlutaMAX, and 1% penicillin/streptomycin (fMSC medium). iMSCs were generated from human fMSCs after establishing an iPSC line [24] and from the ESC line H1 (WiCell Research Institute, Madison, WI) as previously described [25]. Experiments with the human ESC line H1 and the derived iMSCs, and their application in this study were approved by the Robert Koch Institute, Germany (AZ:3.04.02/0132). Briefly, iPSCs and ESCs were cultured without feeder cells on Matrigel (Becton Dickinson, Heidelberg, Germany) using StemMACS iPS-Brew XF, human (Miltenyi Biotec, Bergisch Gladbach, Germany), with 1% penicillin/streptomycin in humidified atmosphere with 5% CO_2 at 37°C, with daily change of medium.

When confluency was reached, the medium was changed to α-MEM (see fMSC medium) and the pluripotent cells were treated daily with 10 μM of the transforming growth factor-β (TGF-β) receptor inhibitor SB-431542 (Miltenyi Biotec) for 14 days. Afterward, the emerged iMSCs were trypsinized using TrypLE Express (Thermo Fisher Scientific, Waltham, MA) for 10 min at 37°C, centrifuged at 300 *g* for 5 min, and seeded onto uncoated culture dishes in an MSC expansion medium (see fMSC medium), which led to the depletion of cells with maintained iPSC characteristics. Further passaging was carried out as described above when cells reached about 95% confluency. The cells were seeded at 1×10^6 cells per 175 cm^2.

Transcriptome analysis

Microarray experiments were performed on the PrimeView Human Gene Expression Array platform (Affymetrix; Thermo Fisher Scientific), the data are provided online at the National Center of Biotechnology Information (NCBI) Gene Expression Omnibus (https://www.ncbi.nlm.nih.gov/geo/query/acc.cgi?acc=GSE97692). The unnormalized bead-summary data were further processed through the R/Bioconductor environment employing the package affy (http://bioconductor.org/packages/release/bioc/html/affy.html). Using this package, the data were background-corrected, transformed to a logarithmic scale (to the base 2), and normalized by applying the Robust Multi-array Average normalization method.

Immunophenotyping by flow cytometry

The cell surface marker expression of the fMSCs and iMSCs was analyzed by using the human MSC Phenotyping Kit Human (# 130-095-198) from Milteny Biotec. To conduct this analysis, 200,000 detached cells were distributed into two 5 mL flow cytometry tubes in 100 μL phosphate-buffered saline (PBS). The phenotyping cocktail (0.5 μL) containing antibodies against CD14-PerCP, CD20-PerCP, CD34-PerCP, CD45-PerCP, CD73-APC, CD90-FITC, and CD105-PE or the isotype control cocktail was then applied. After 10 min of incubation at 4°C, the cells were washed and resuspended in 100 μL paraformaldehyde (PFA 4%) for flow cytometric analysis (FACS Canto from BD Biosciences, Heidelberg, Germany). The histograms were generated using the FlowJoV10 Software (FlowJo LLC, Ashland, OR).

Trilineage differentiation of MSCs

Differentiation of the fMSCs and iMSCs into adipocytes, chondrocytes, and osteoblasts was carried out for 3 weeks using the STEMPRO Adipogenesis/Chondrogenesis/Osteogenesis Differentiation Kit (Thermo Fisher Scientific). Afterward, the cells were fixed with PFA (4%) and stained with 0.2% Oil Red O (adipocyte differentiation), 1% Alcian Blue (chondrocyte differentiation), or 2% Alizarin Red S (osteoblast differentiation) solutions according to standard protocols.

Cell proliferation analyses

The cell proliferation capacity of the fMSCs, iPSC-iMSCs, and ESC-iMSCs was measured by the incorporation of bromodeoxyuridine (BrdU) using the cell proliferation enzyme-linked immunosorbent assay (ELISA), BrdU (colorimetric) kit (Roche, Basel, Switzerland), according to the manufacturer's instructions. The cells were seeded at 30,000 cells per well in a 96-well flat-bottom plate in triplicates. BrdU (100 μM) was added 24 h later for an incorporation time of 21 h. Cells were fixed, BrdU antibodies coupled with peroxidase were added for 90 min, and the substrate applied for 30 min. The colorimetric reaction was measured using an

ELISA reader (Biotech Instruments, Heilenpark, Germany) (dual, wavelength 655–490 nm).

Short tandem repeat analysis

The genetic background of cells was analyzed by short tandem repeat (STR) using genomic DNA. For isolation of genomic DNA, the GeneMATRIX DNA/RNA/Protein Universal Purification Kit (Roboclon, Berlin, Germany) was used. For polymerase chain reaction (PCR), 5 μL 1× Go-Taq G2 Hot Start Green PCR buffer, 4 mM $MgCl_2$, 0.5 μL dNTP Mix (10 mM each), 1 μL forward primer (0.3 μM), 1 μL reverse primer (0.3 μM) (sequences are given in Supplementary Table S1; Supplementary Data are available online at www.liebertpub.com/scd), 0.125 μL (0.625 U) Hotstart Taq Polymerase (5 U/μL), and 100 ng genomic DNA were mixed. Water was added to adjust a final volume of 25 μL. The PCR was performed in a thermal cycler (PEQLAB, Erlangen Germany) starting with 5 min of initial denaturation at 94°C followed by 32 cycles comprising a denaturation step at 94°C for 15 s, an annealing step at 60°C for 30 s, and an extension step at 68°C for 60 s (D7S796 and D21S2055). For other STR primers, the PCR program was used as described [26]. Detection of PCR amplification products was done by gel electrophoresis (2.5% agarose gels).

Liver injury model and cell transplantation

Gunn rats with mutated *Ugt1a1* [6] were obtained from the Rat Resource & Research Centre (RRRC, Columbia, MO) and maintained at the animal facility of the Heinrich Heine University (Düsseldorf, Germany). Immunocompetent female Gunn rats with homozygous mutation were anesthetized by combined ketamine (100 mg/kg) and xylazine (10 mg/kg) injection and the two largest liver lobes were surgically removed (70% of the liver, partial hepatectomy [PHX]) essentially as described [27]. Immediately after PHX, while the abdomen was still open, ~4 million fMSCs ($n=4$), ESC-iMSCs ($n=3$), or iPSC-iMSCs ($n=3$) from male human donors were transplanted into rats through the spleen. For this, the cells were trypsinized, resuspended in 300 μL Ringer lactate buffer, filtered through a mesh (40 μm), and injected into the tip of the spleen using G30 syringes. One rat (T7) that received iPSC-iMSCs showed internal bleeding in the uterus with low bilirubin serum levels and was, therefore, excluded from further analysis. Control Gunn rats underwent PHX ($n=4$), but received no cell transplantation. After 2 months of recovery, the animals were sacrificed by loss of blood during anesthesia. The livers were then perfused with physiologic buffer and snap-frozen in liquid nitrogen. The animal experiments were approved by the relevant federal state authority for animal protection (Landesamt für Natur, Umwelt und Verbraucherschutz Nordrhein-Westfalen, Recklinghausen, Germany; Reference No. 84-02.04.2012.A344).

Serum and culture supernatant analysis

To determine the presence of albumin (ALB) in the blood of Gunn rats 2 months after transplantation of human iMSCs and control animals, the blood was collected from the portal vein and diluted 1:10,000. Human serum samples from three individuals were diluted 1:1,000,000, whereas culture supernatants from fMSCs and iMSCs were taken without dilution. These samples were analyzed by an ELISA specific for human ALB according to the manufacturer's recommendations (human ELISA quantitation set, # E80-129; Bethyl Laboratories, Montgomery). The concentration of total ALB, lactate dehydrogenase (LDH), alanine transaminase (ALT), and aspartate transaminase (AST) in the serum was quantified by a Spotchem EZ SP-4430 using diagnostic test strips for multiparameter analysis (# 77182; Arkray Europe, Amstelveen, Netherlands). The concentration of total bilirubin in the serum was measured using the colorimetric Bilirubin Assay kit (MAK126; Sigma-Aldrich). A cytokine array was performed according to the protocol from Proteome Profiler Human Cytokine Array Panel A (R&D Systems) using 0.4 mL of Gunn rat serum. The emitted chemiluminescence was analyzed by measuring the pixel density of each spot on the array membrane, including reference and negative control spots.

Analysis of bile acids and their conjugates

Bile acids were analyzed by ultra-high performance liquid tandem mass spectrometry (UHPLC-MS/MS) essentially as described [28]. The system consists of a UHPLC-I class (Waters, United Kingdom) coupled to a Xevo TQ-S triple quadruple mass spectrometer (Waters). Electrospray ionization was performed in the negative ionization mode. Chromatographic separation was performed on a BEH C18 column (2.1 × 100 mm, 1.7 μm). The mobile phase consisted of water containing 0.1% formic acid and 5 mM ammonium acetate (Eluent A) and acetonitrile (Eluent B). Analytes were separated by gradient elution. The injection volume was 5 μL and the column was maintained at 40°C. Detection of the bile acids and their glycine and taurine conjugates was performed in selected reaction monitoring mode. All standards as well as the deuterated internal standard substance (d4-CA, d4-GCA and d5-TCA) were purchased from Sigma-Aldrich and Steraloids (Newport).

Reverse transcriptase-PCR

Human-specific primers (Supplementary Table S1) were generated to detect human mRNA in Gunn rat liver. Total RNA was isolated from five different liver pieces of each rat using the RNeasy Mini kit (Qiagen, Hilden, Germany) according to the manufacturer's recommendations. First-strand cDNA was made from 1 μg total RNA per 20 μL reaction volume (RevertAid H Minus First Strand cDNA Synthesis Kit; Thermo Fisher Scientific). A standard protocol using the 2×PCR Master Mix (Thermo Fisher Scientific), 0.8 μM primers, and 5 μL template cDNA per 25 μL reaction volume was used to obtain PCR products by conventional PCR. For quantitative real-time PCR (qPCR), 12.5 ng cDNA per sample, 0.6 μM primers, and the Power Sybr Green Master Mix (Life Technologies) were used. Universal β-actin primers for humans and rats served as a reference gene for the normalization of values calculated by the $2^{-\Delta\Delta Ct}$ method. Human samples of normal liver tissue from patients with tumors were used as a reference to assess the abundance of iMSC-derived cells within Gunn rat tissue. A written consent was given by the patients and the usage of

liver samples for research was approved by the local ethics committee of the Medical Faculty of the Heinrich Heine University Düsseldorf (Germany).

Immunohistochemistry and immunofluorescence analysis

For immunohistochemistry, tissue sections were made from frozen livers and fixed with 4% formalin for 20 min. The fixed sections were treated with 0.1% Triton X-100, washed in PBS, and endogenous peroxidases were blocked (dual endogenous enzyme block, # S2003; Dako, Glostrup, Denmark). Unspecific binding of antibodies was prevented by the treatment with 10% FBS in PBS supplemented with 0.1% saponin. A mouse antibody against the human cytosolic protein Stem121 (# Y40410; Takara Bio USA, Mountain View, CA) and anti-mouse immunoglobulins coupled with horseradish peroxidase (# AP192P; Merck Millipore, Darmstadt, Germany) were used for diaminobenzidine (DAB) staining (# K346711-2; Dako). The cell nuclei were counterstained by diluted hematoxylin solution (1:5, # 1.05175.0500; Merck Millipore). For the identification of liver cell types, DAB-stained sections were treated with monoclonal antibodies against CK18 (# BM2275P; Acris, Herford, Germany) or HNF4α (# 3113; Cell Signaling, Danvers, MA). The primary antibodies were then labeled by Cy3-conjugated secondary antibodies directed against mouse or rabbit immunoglobulins (# AP192C, # AP182C; Merck-Millipore). Antibodies against Collagen 1 (# C2456; Sigma-Aldrich), Collagen 4 (# ab6586; Abcam, Cambridge, United Kingdom), OCT4-A (# C30A3; Cell Signaling), and PDGFRβ (# 3169S; Cell Signaling) were used for immunofluorescence of liver sections and cultured cells. The sections were fixed with ice-cold methanol, whereas 4% PFA was used to fix cultured cells. Appropriate secondary Cy3-, FITC-, or Alexa Fluor 555-labeled antibodies (# AP182C/F, # AP192C/F; Merck-Millipore, # A-21428; Thermo Fisher Scientific) and 4′,6-diamidino-2-phenylindole (DAPI Fluoromount G, # 0100-20; Southern Biotech, Birmingham, AL) or Hoechst 33258 dye (1:5,000; Sigma-Aldrich) were applied to mark primary antibodies and cell nuclei, respectively.

Fluorescence in situ hybridization

Fluorescence in situ hybridization (FISH) was carried out after fixation of liver cryosections with Carnoy's solution (75% methanol and 25% acetic acid) followed by pepsin digestion (0.05 mg/mL pepsin from Roche in 0.01 N chloric acid). Human-specific Y chromosome probe (#D-0324-100-OR; MetaSystems, Altlußheim, Germany) and rat-specific X chromosome probe (#IDRF1067; Empire Genomics, Buffalo, NY) were dissolved in a hybridization solution (Empire Genomics) and hybridized with the sections overnight at 37°C after an initial denaturation at 75°C. After washing with saline sodium citrate, the sections were covered with a mounting medium (DAPI Fluoromount G; Southern Biotech).

Statistics

All data were indicated as arithmetic mean ± standard error of mean. Statistical analysis was performed by Student's *t*-test and ANOVA (analysis of variance). *P* values of <0.05 were considered significant and indicated by different letters in the graphs.

Results

Human ESC- and iPSC-derived iMSCs are functional MSCs

Human iMSCs were derived from the ESC line H1 (ESC-iMSCs) and iPSCs from fetal MSCs (iPSC-iMSCs) by inhibition of TGF-β signaling with SB-431542 for 14 days. This treatment resulted in the downregulation of the pluripotency-regulating octamer-binding transcription factor 4 (OCT4), resulting in the acquisition of the typical fibroblast-like cell morphology as well as expression of MSC surface markers such as PDGFRβ (Fig. 1A). The transcriptomes of iMSCs from both sources were compared with the transcriptomes of iPSCs, ESCs, and fMSCs by microarray analysis (Fig. 1B). The iMSCs from ESCs and iPSCs expressed molecular markers typical of MSCs, namely *CD44*, *CD73*, *CD105*, *CD146*, and *PDGFRβ*. In addition, expression of pluripotency-regulating transcription factors—*OCT4*, SRY (sex-determining region Y)-box 2 (*SOX2*), and *NANOG*—was downregulated in iMSCs both at the mRNA and protein level (Fig. 1A, B). In line with this, Pearson correlation analysis of the transcriptome data showed a low correlation of iMSCs with their pluripotent precursor cells and high correlation (R^2 values 0.944 and 0.966) with fMSCs (Fig. 1C), which was also mirrored by cluster analysis (Supplementary Fig. S1A). STR analysis confirmed the same genetic background for (1) fMSCs, iPSCs, and iPSC-iMSCs, and (2) ESC and ESC-iMSCs, as indicated by distinct banding patterns (Supplementary Fig. S1B).

Flow cytometry-based analysis revealed comparable MSC surface marker expression (CD73, CD90, and CD105) in iMSCs and fMSCs (Fig. 2A–I), and markers of hematopoietic cells were absent (Fig. 2J–L). Statistical analysis revealed no significant differences between iMSCs and the fMSCs with respect to these cell surface markers. Furthermore, the fMSCs as well as the iMSCs displayed a spindle-shaped, fibroblast-like morphology (Fig. 3A1–A3). Similar to fMSCs, iMSCs from ESCs and iPSCs were observed to differentiate into adipocytes with characteristic fat droplets following treatment with an adipocyte differentiation medium, as evidenced by Oil Red O staining (Fig. 3B1–B3). A typical differentiation along the chondrogenic and osteogenic cell lineages was demonstrated for iMSCs, as seen in fMSCs (Fig. 3C1–D3). A BrdU ELISA was performed to determine the relative cell proliferation capacity showing that fMSCs were significantly more proliferative than iPSC-iMSCs and ESC-iMSCs, whereas no significant difference was observed when the two iMSC populations were compared (Supplementary Fig. S2).

The iMSCs neither expressed nor secreted human ALB as investigated by transcriptome analysis and an ELISA specific for human ALB (Fig. 4A, B). In addition, other hepatocyte-specific markers such as hepatocyte nuclear factor 4α (*HNF4α*), *UGT1A1*, bile salt export pump (*BSEP*), multidrug resistance protein 2 (*MRP2*), Na/taurocholate-cotransporting polypeptide (*NTCP*), and α-fetoprotein (*AFP*) were also not expressed. In contrast to this, connective tissue proteins such as collagens (*COL1α2*, *COL4α1*), connective tissue growth factor, and α-smooth muscle actin (*α-SMA*) were detected at the mRNA level (Fig. 4A).

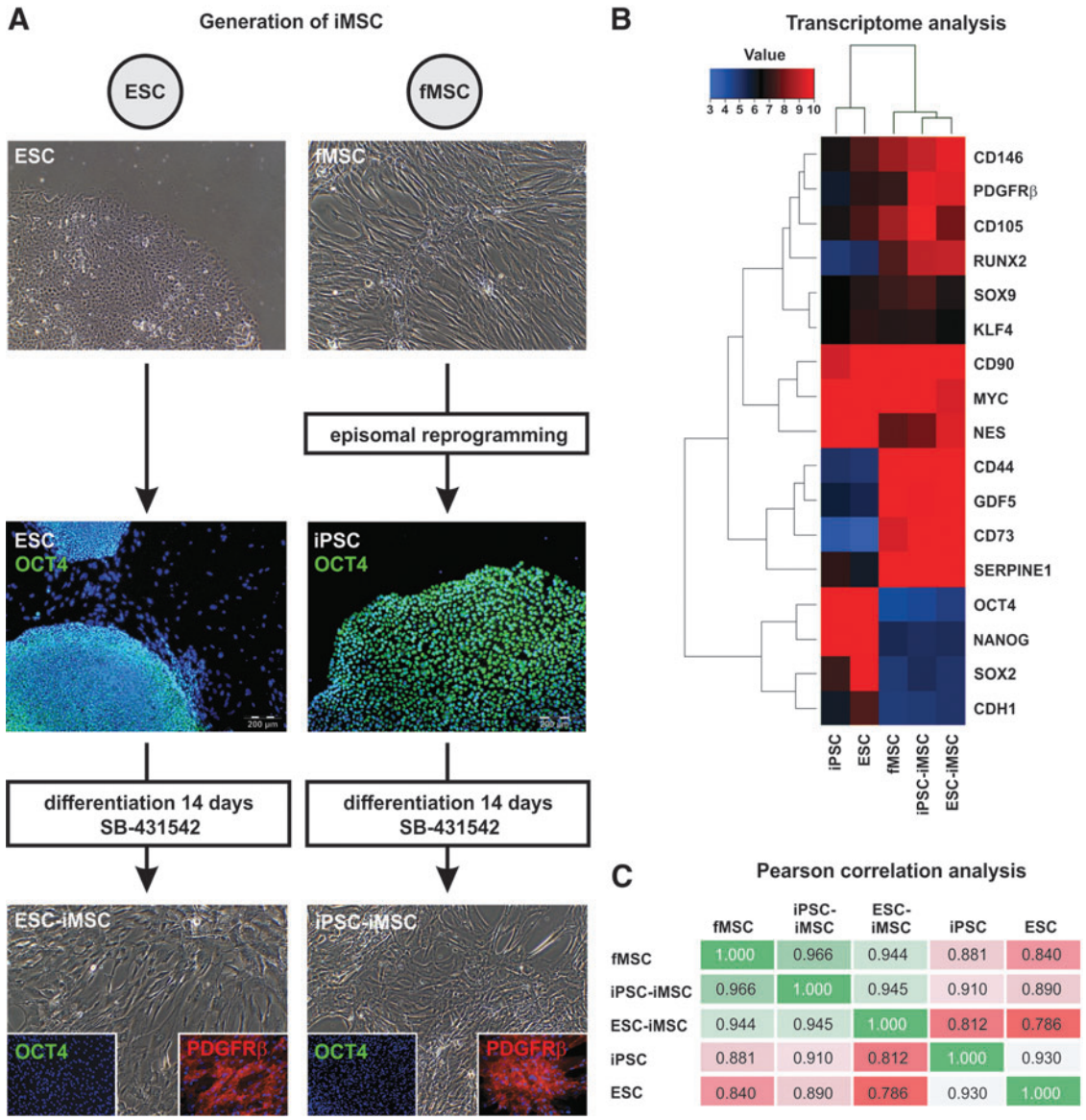

	fMSC	iPSC-iMSC	ESC-iMSC	iPSC	ESC
fMSC	1.000	0.966	0.944	0.881	0.840
iPSC-iMSC	0.966	1.000	0.945	0.910	0.890
ESC-iMSC	0.944	0.945	1.000	0.812	0.786
iPSC	0.881	0.910	0.812	1.000	0.930
ESC	0.840	0.890	0.786	0.930	1.000

FIG. 1. Characterization of iMSCs by immunofluorescence and transcriptome analysis. **(A)** Scheme of iMSC generation from the human ESC line H1 and fMSCs. ESCs expressing the pluripotency-associated marker OCT4 were treated with the TGF-β receptor inhibitor SB-431542 for 14 days to facilitate their differentiation into iMSCs, concomitant with the loss of OCT4 expression and the appearance of fibroblast-shaped cells expressing the MSC marker PDGFRβ. To generate iMSCs from fMSCs, the cells were first reprogrammed into pluripotent OCT4-expressing iPSCs using plasmids encoding the pluripotency factors *OCT4*, *SOX2*, *c-MYC*, *KLF4*, *NANOG*, and *LIN28*. After treatment with SB-431542, the iPSCs differentiated into $OCT4^{-}/PDGFR\beta^{+}$ iMSCs as observed for ESC-iMSCs. Cell nuclei were stained with Hoechst 33258 (*blue*), OCT4 with FITC (*green*), and PDGFRβ with Cy3 (*red*). **(B)** ESC- and iPSC-derived iMSCs were characterized by gene expression array analysis (Euclidean correlation analysis). The transcriptome analysis was performed once for a representative preparation of each cell type. **(C)** Pearson correlation analysis of these transcriptome data revealed a high correlation (*green*) of both iMSCs with fMSCs, but low correlation (*red*) with their pluripotent precursors (ESCs and iPSCs). Scale bars indicate 200 μm. ESC, embryonic stem cell; fMSC, fetal mesenchymal stem cell; iMSC, induced mesenchymal stem cell; iPSC, induced pluripotent stem cell; OCT4, octamer-binding transcription factor 4; PDGFRβ, platelet-derived growth factor receptor β; SOX2, SRY (sex-determining region Y)-box 2; TGF-β, transforming growth factor-β.

Engraftment and differentiation of transplanted iMSCs

After surgical removal of about 70% of the liver (partial hepatectomy/PHX), ESC-iMSCs, iPSC-iMSCs, or fMSCs were immediately transplanted into Gunn rats with homozygous *Ugt1a1* mutation through spleen injection without immunosuppression. The rats were allowed to recover from liver injury over 2 months, to investigate long-term effects of transplanted human iMSCs. Afterward, engraftment of transplanted ESC- and iPSC-iMSCs was seen in five out of six animals (83%) by analysis of human ALB in Gunn rat blood serum as shown by human-specific ELISA for ALB, whereas ALB was not released by cultured iMSCs (Fig. 4B,

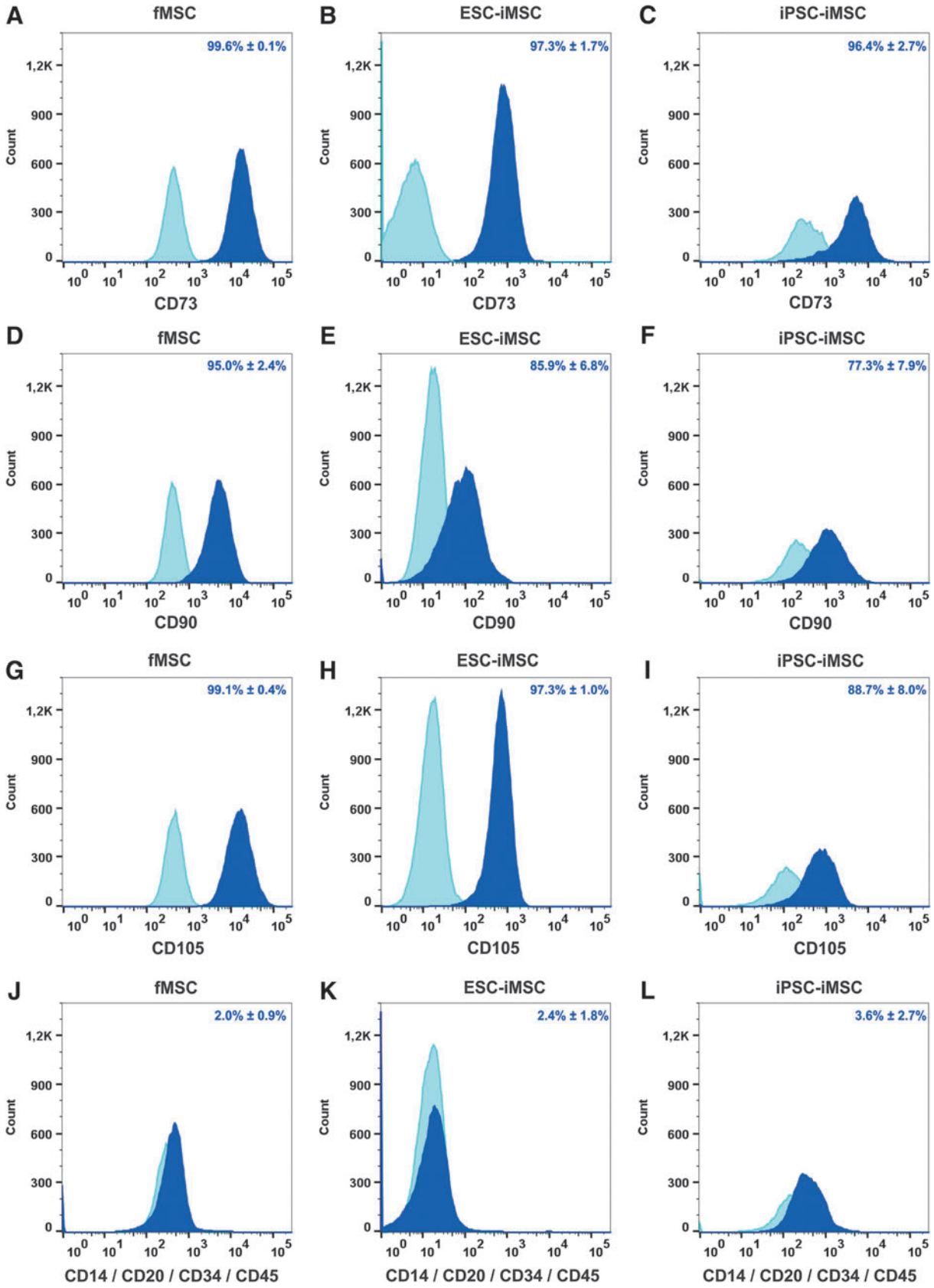

FIG. 2. Characterization of fMSCs and iMSCs by flow cytometry. The MSC markers **(A–C)** CD73, **(D–F)** CD90, and **(G–I)** CD105 were detectable as cell surface proteins on fMSCs and iMSCs derived from ESCs and iPSCs, whereas the expression of hematopoietic markers **(J–L)** CD14, CD20, CD34, and CD45 was low (*dark blue*). *Light blue* histograms represent antibody isotype controls. Representative data of repeated analysis of each cell type are shown (fMSCs $n=4$; ESC-iMSCs $n=3$; and iPSC-iMSCs $n=4$). The percentage of positive cells for particular cell surface markers is indicated as a mean ± SEM of different analysis. SEM, standard error of mean.

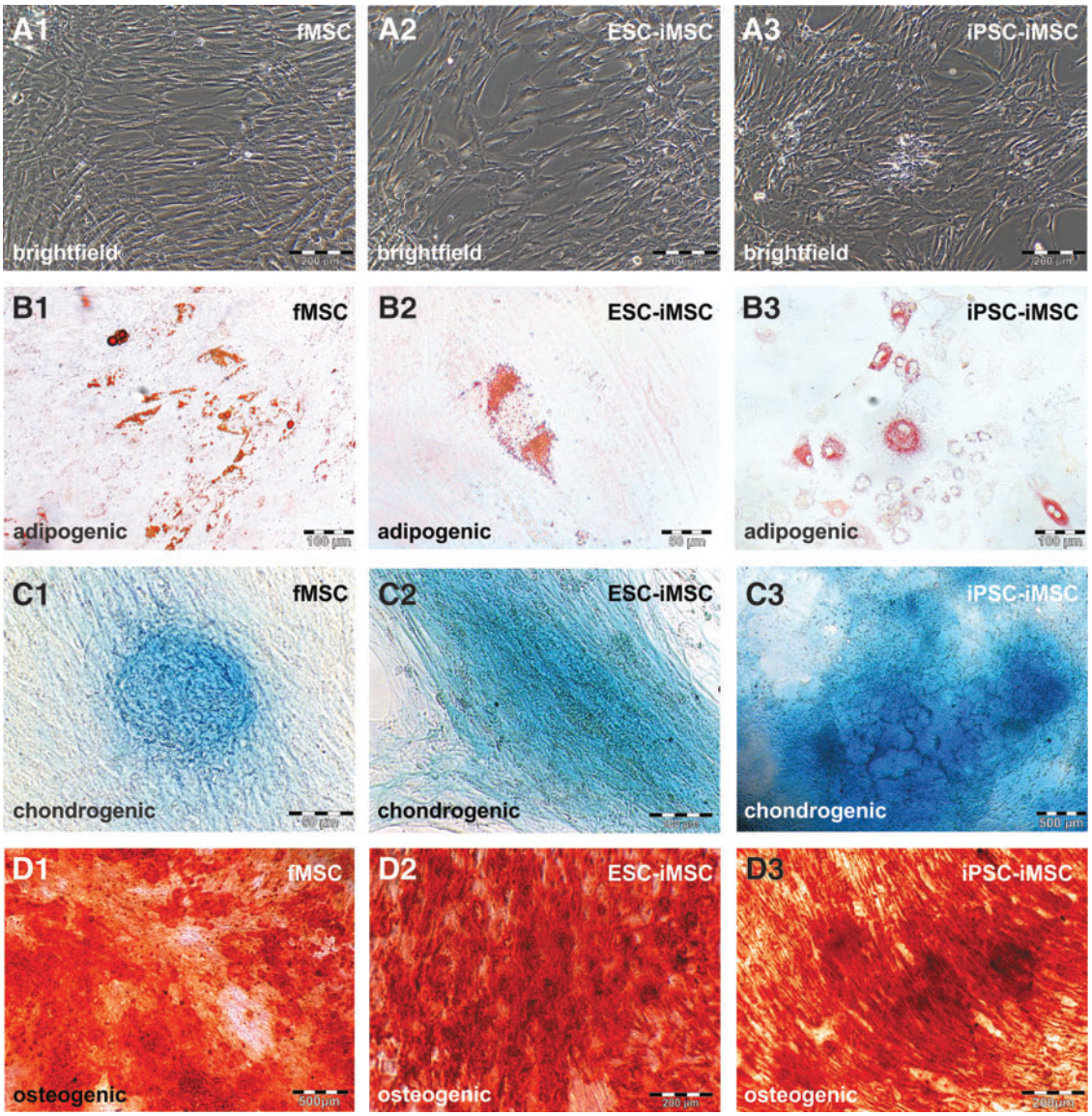

FIG. 3. Functional characterization of fMSCs and iMSCs. To test the developmental potential of iMSCs by qualitative assays, differentiation media for adipogenic (fMSC: $n=7$; ESC-iMSC: $n=3$; and iPSC-iMSC: $n=3$), chondrogenic (fMSC: $n=2$; ESC-iMSC: $n=3$; and iPSC-iMSC: $n=2$), and osteogenic (fMSC: $n=5$; ESC-iMSC: $n=3$; and iPSC-iMSC: $n=3$) development were applied for 21 days. **(A1–D1)** fMSCs and iMSCs **(A2–D2,** ESC-iMSCs; **A3–D3,** iPSC-iMSCs) showed **(A1–A3)** fibroblast-like morphology and were able to differentiate into **(B1–B3)** adipocytes (Oil Red O-stained lipid droplets), **(C1–C3)** chondrocytes (Alcian Blue 8GX marked glycosaminoglycans in cartilage), and **(D1–D3)** osteoblasts (Alizarin Red stained calcium deposits). Scale bars indicate 50 μm **(B2, C1)**, 100 μm **(B1, B3, C2)**, 200 μm **(A1–A3, D2, D3)**, and 500 μm **(C3, D1)**.

C). Approximately 1%–4% (0.03–0.13 g/dL) of total albumin (rat and human) was of human origin. The total albumin concentration in the transplantation and control groups remained unchanged at 3.2 g/dL. Transplanted iPSC-iMSCs showed lower ALB concentrations in host rat serum (Fig. 4C) and one animal of this group exhibited no signs of engraftment (Supplementary Table S2). Engraftment of transplanted fMSCs was only found in one of four rats and, therefore, not included in detailed analysis (Supplementary Table S2).

To determine the effects of transplanted iMSCs on the disease phenotype of Gunn rats, total bilirubin concentration was measured and found to be reduced by ~31% (ESC-iMSCs) and 22% (iPSC-iMSCs) in Gunn rats of the transplanted groups compared to control (Fig. 4D), indicating partially suppressed hyperbilirubinemia.

The presence of human ALB in the sera of Gunn rats after iMSC transplantation was confirmed at the mRNA level by qPCR employing human-specific primers (Fig. 5A). The relative amount of human *ALB* mRNA in Gunn rat liver was ~2%–3% when mRNA samples of human liver tissues were used as a reference and set to 100% (Fig. 5A). However, the abundance of human *ALB*-expressing cells was found to be variable in distinct areas of each single liver and varied between 0% and 18%. The expression of human hepatocyte markers within rat liver tissue was further detected by human-specific primer sets for *UGT1A1,*

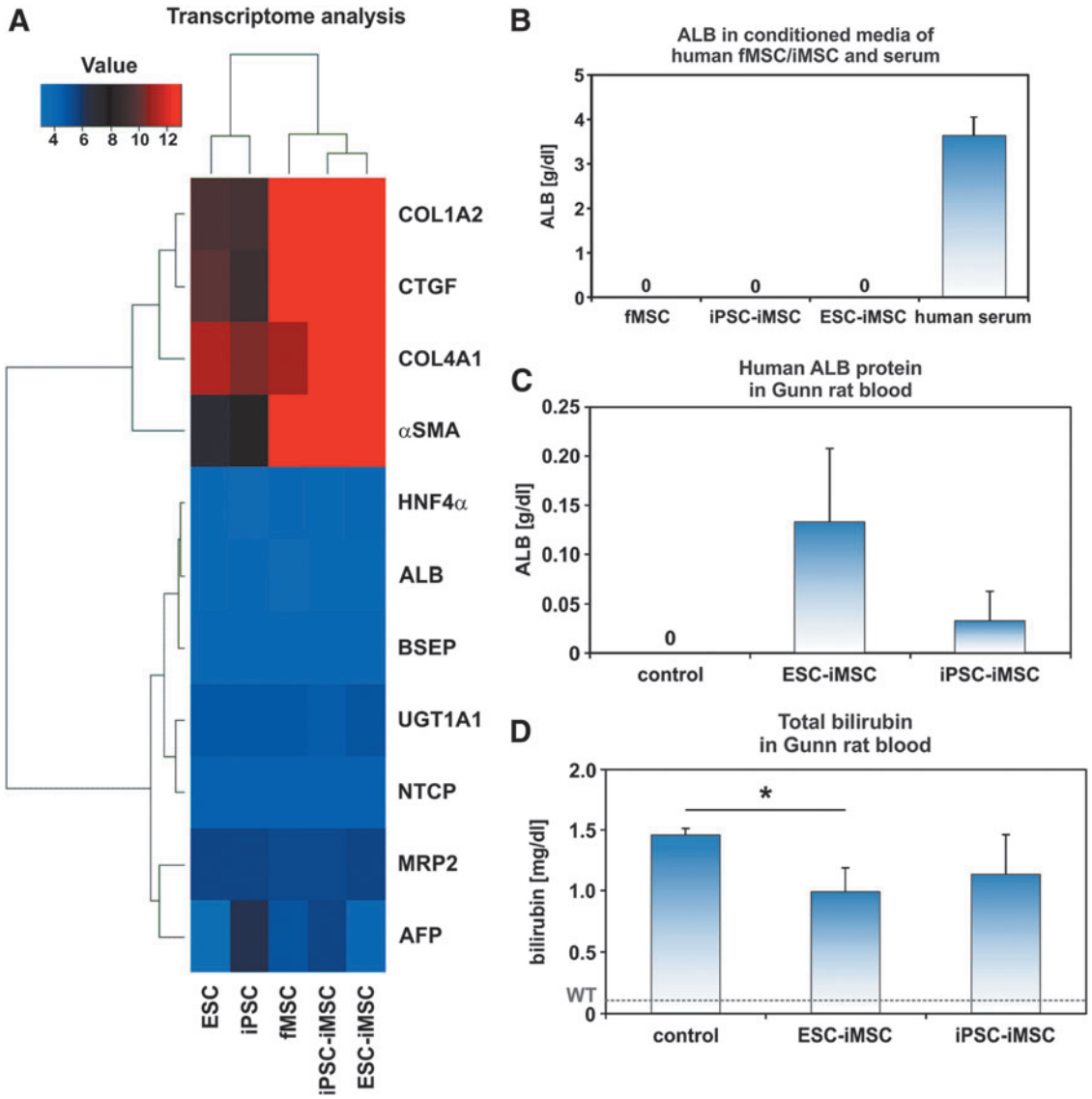

FIG. 4. Transplanted human iMSCs acquired hepatocyte functions in host Gunn rats. **(A)** Transcriptome analysis confirmed the lack of hepatocyte marker expression in pluripotent stem cells as well as fMSCs and iMSCs before transplantation, but indicated an expression of connective tissue markers and α-*SMA* (Euclidean correlation analysis), which are typically expressed by MSCs. The transcriptome analysis was performed once for a representative preparation of each cell type. **(B)** Moreover, cultured fMSCs and iMSCs did not secrete ALB into the culture medium as determined by a human-specific ALB ELISA. The normal level of ALB in human blood serum of healthy volunteers is indicated as a mean (3.6 g/dL; $n=3$). **(C)** A differentiation of the transplanted human ESC-iMSCs and iPSC-iMSCs into hepatocytes was indicated by the presence of human ALB within the serum of Gunn rats. **(D)** The total bilirubin concentration in blood significantly decreased in Gunn rats after transplantation of human ESC-iMSCs, but reached no significance for iPSC-iMSCs **(C, D:** control $n=4$; ESC-iMSC: $n=3$; iPSC-iMSC: $n=3$; $^*P<0.05$). The mean bilirubin level of normal wild-type rats (WT, 0.1 mg/dL) is indicated by a *broken line* [29]. ALB, albumin; α-SMA, α-smooth muscle actin; ELISA, enzyme-linked immunosorbent assay.

HNF4α, *BSEP*, *NTCP*, *MRP2*, cytochrome P450 1A2 (*CYP1A2*), *CYP2D6/7*, and *CYP3A4/5/7* (Fig. 5B–I). Accordingly, these hepatocyte-specific mRNAs reached comparable amounts as observed for *ALB* mRNA. The mean value for human *AFP*, a marker for immature hepatocytes, was ~2%–8% (Fig. 5J), and human hypoxanthine phosphoribosyl transferase 1 (*HPRT1*) as a housekeeping gene for human cells reached 16% (ESC-iMSCs) and 7% (iPSC-iMSCs) in Gunn rat liver (Fig. 5K). This suggested that, in addition to mature and immature hepatocytes, other human cells were present in the Gunn rat livers. Indeed, expression of the MSC marker *CD105* was detectable, indicating persisting human iMSCs (Fig. 5L). To find additional evidence for the presence of human iMSCs, sera from Gunn rats of the transplantation groups and control were analyzed for the presence of human cytokines, employing secretome arrays. Human RANTES (CC motif ligand 5) and SERPIN Family E Member 1 (SERPINE1) could only

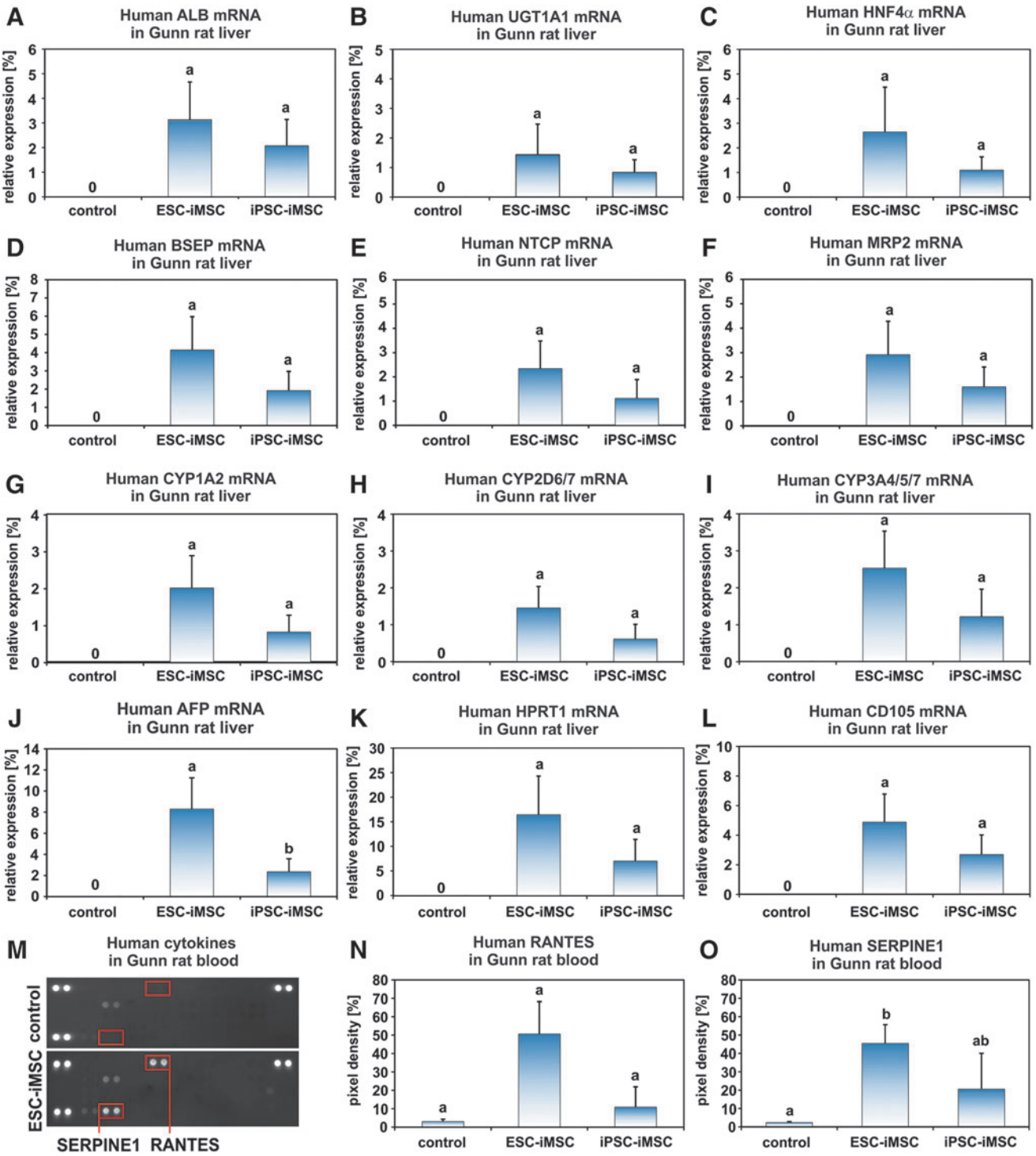

FIG. 5. Transplanted human iMSCs successfully engrafted in Gunn rat liver and expressed hepatocyte markers. Gunn rat liver tissue and serum were analyzed 2 months after iMSC transplantation. **(A)** The presence of human *ALB* transcripts within Gunn rat liver was analyzed by qPCR. Additional hepatocyte-associated genes such as **(B)** *UGT1A1*, **(C)** *HNF4α*, **(D)** *BSEP*, **(E)** *NTCP*, **(F)** *MRP2*, **(G)** *CYP1A2*, **(H)** *CYP2D6/7*, **(I)** *CYP3A4/5/7*, and **(J)** *AFP* were found by human-specific primers for qPCR. The results were normalized to human liver samples, which were set to 100%. Thus, the bars represent proportions of the expression values of human liver. **(K)** Human-specific primers for *HPRT1* were used to assess the total abundance of human cells derived from iMSCs. **(L)** The MSC marker *CD105* remained detectable by human-specific primers in qPCR within the host Gunn rat livers. **(M)** Human RANTES and SERPINE1 were detected by protein arrays in the serum of Gunn rats transplanted with human iMSCs. A representative blot of the control and one transplantation group is shown. The three spot pairs in the *corners* represent protein array quality controls. Densitometric analysis of **(N)** RANTES and **(O)** SERPINE1 spots (highlighted by *red boxes*). The small bar of the control group represents the background pixel density (pixel density in % to the control spots). **(A–I, K–L:** control $n=4$, ESC-iMSC, passage 10, $n=3$; iPSC-iMSC, passage 10, $n=3$, groups without significant differences share similar letters; $P<0.05$). *AFP*, α-fetoprotein; *BSEP*, bile salt export pump; *HNF4α*, hepatocyte nuclear factor 4α; *MRP2*, multidrug resistance protein 2; *NTCP*, Na/taurocholate-cotransporting polypeptide; qPCR, quantitative real-time polymerase chain reaction; *Ugt1A1*, uridine diphosphate glucuronosyltransferase-1a1.

be detected in the serum of the transplantation groups (Fig. 5M–O), indicating the presence of cytokine-secreting human cells.

Histological analysis of Gunn rat liver

To identify iMSC-derived cells within Gunn rat liver tissue, the human-specific antibody Stem121 directed against a cytoplasmic protein was used for immunohistochemistry analysis (Fig. 6). Stem121-positive cells were mainly located within the rat liver tissue around the central vein zone 3 and 2, as observed after iMSC transplantation (Fig. 6B, C). These cells were polygonal shaped with one or two cell nuclei, which is typical for hepatocytes (Fig. 6C, D1–F1). Costaining of Stem121 immunohistochemistry with fluorescence-labeled antibodies directed against the hepatocyte markers CK18 and HNF4α further indicated cells with hepatocyte characteristics of human origin (Fig. 6D3–F3). To investigate possible cell fusion events after iMSC transplantation, human-specific Y chromosome probes were combined with rat-specific X chromosome probes in FISH analysis, since pluripotent cells from male donors were used for the generation of iMSCs. Besides cells bearing the Y chromosome, cells with both human Y and rat X were found, indicating fusion of human-derived cells with rat cells in Gunn rat livers after transplantation (Supplementary Fig. S3).

Seemingly, human iMSC-derived hepatocytes were present in Gunn rats and, therefore, we examined and quantified the bile acid composition in rat blood serum using UHPLC-MS/MS, to determine any increase in glycine-conjugated bile acids, typical in human serum. The sum of unconjugated bile acids was increased in the iMSC groups compared to the control group. However, the concentrations of taurine- and glycine-conjugated bile acids were not significantly altered between the groups (Supplementary Fig. S4). To search for adverse effects as a consequence of iMSC transplantation, their possible contribution to fibrosis was analyzed by immunofluorescence and qPCR. As shown by representative immunofluorescent images of Collagen 1 and 4 (Supplementary Fig. S5), no significant scar formation was observed in liver sections of the transplanted groups compared to the control group. In line with this, upregulation of Collagen 1 and α-SMA mRNA was not found in host Gunn rat livers (not shown). However, the relative amount of Collagen 4 mRNA increased significantly by $85\% \pm 15\%$ ($P < 0.05\%$) after ESC-iMSC transplantation, but reached no significance for iPSC-iMSCs. To identify adverse effects imparted by the transplanted iMSCs, serum concentrations of LDH, ALT, and AST were investigated, but these values were not significantly different between the transplanted and control groups (Supplementary Table S2), suggesting no immediate obvious adverse effects by transplanted iMSCs.

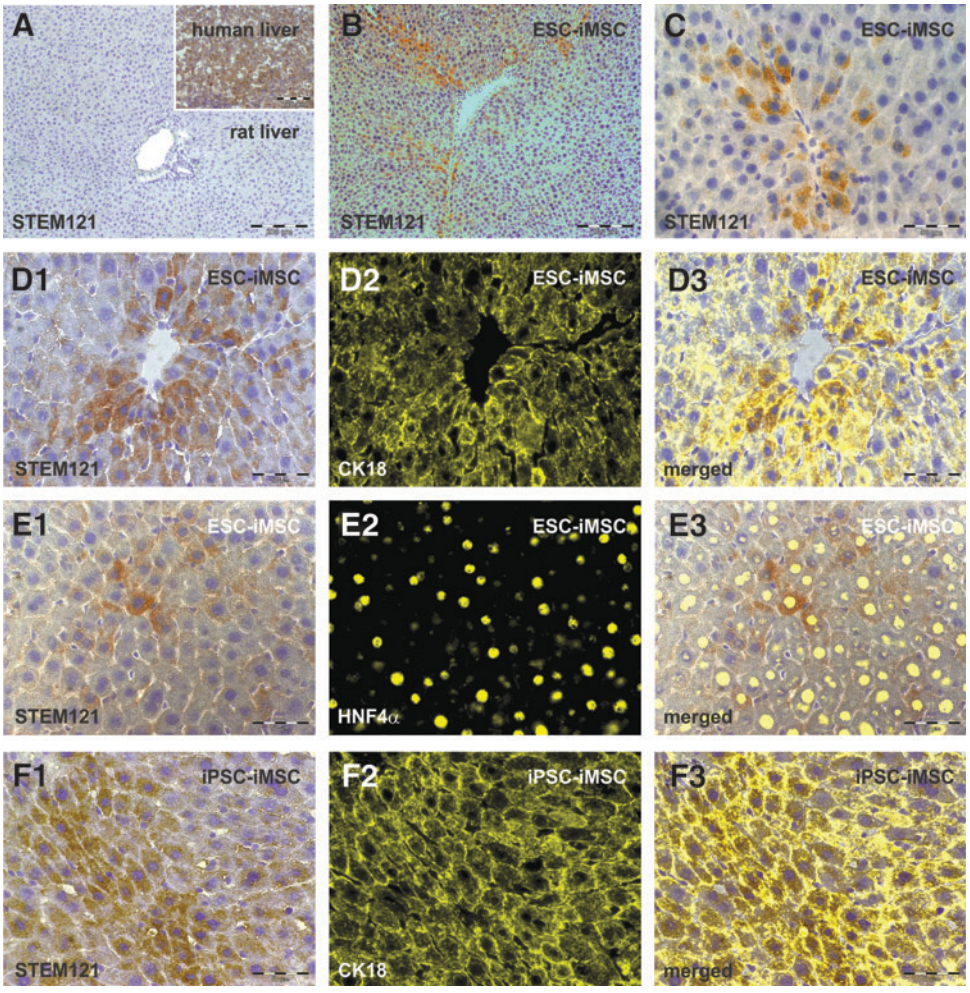

FIG. 6. Histological analysis of human iMSC-derived hepatocytes within the Gunn rat liver. Gunn rat liver tissues were analyzed by immunohistochemistry of the human cytoplasmic protein Stem121 by DAB staining (*brown*) 2 months after iMSC transplantation. Liver sections of control Gunn rats 2 months after PHX showed no specific Stem121 antibody binding, whereas human liver tissue exhibited intense Stem121 DAB staining, indicating its specificity for human cells **(A** with *insert*; $n = 4$). Stem121 DAB staining was also combined with immunofluorescence of the hepatocyte markers CK18 or HNF4α (*yellow*). Human iMSC-derived hepatocytes with positive Stem121 staining were found after transplantation of **(B–E3)** ESC-iMSCs and **(F1–F3)** iPSC-iMSCs (passage 10, $n = 3$). The presence of Stem121 together with CK18 or HNF4α confirms the presence of hepatocytes of human origin. Scale bars indicate 50 μm **(C–F3)** and 200 μm **(A, B)**. DAB, diaminobenzidine; PHX, partial hepatectomy.

Discussion

Human MSCs are widely used in clinical trials and research studies. In a clinical scenario, however, MSCs are often obtained from elderly patients and may have lost their original properties due to changes within the stem cell niches [30]. Moreover, negative influences by prolonged culture without appropriate stem cell niche in vitro could lower their potential to proliferate and differentiate, thereby limiting their therapeutic outcome. Generation of iPSC-derived iMSCs from individual patients may overcome some of these disadvantages and offer significant potential and basis for personalized medicine.

Thus, to date, studies have shown that MSCs generated from either iPSCs or ESCs acquire a rejuvenated phenotype with high proliferative capacity capable of enhancing their therapeutic potential [15–20], and even could outperform primary MSCs [16,17]. We have demonstrated in this study that, iMSCs are similar to fMSCs with respect to their gene expression profile, morphology, cell surface markers, and trilineage differentiation potential at least in vitro. Given their pluripotent origin, it is important to show that iMSCs as derivatives of ESCs and iPSCs are not pluripotent and, thus, do not exhibit tumor formation potential. Expression of *OCT4*, *SOX2*, and *NANOG* was not detected in the iMSCs used in this study and no evidence of tumor formation was found. In contrast, we observed the ability of iMSCs to home into the injured liver and to acquire properties of hepatocytes as indicated by coexpression of human Stem121 (an antibody directed against a human-specific epitope) and hepatocyte markers (CK18 and HNF4α), as well as the release of ALB into the blood and expression of hepatocyte-associated genes such as *ALB, AFP*, *UGT1A1*, *BSEP*, *NTCP*, *MRP2*, *CYP1A2*, *CYP2D6/7*, *CYP3A4/5/7*, and *HNF4α*. To our knowledge, this is the first study showing the contribution of human iMSCs to liver regeneration. In contrast to this, native fMSCs showed poor contribution to liver regeneration compared to iMSCs. The fMSCs were more proliferative than their iMSC counterparts, which could explain their low differentiation potential since these two processes can influence developmental fate decisions of stem cells. Future studies, including comparative analysis of fetal and adult MSCs as well as iMSCs, will be necessary to investigate possible opposing effects of cell proliferation and differentiation.

The Gunn rat is a well-established model for investigating inherited liver diseases such as Crigler-Najjar syndrome 1, characterized by elevated levels of serum bilirubin caused by the *Ugt1a1* mutation [6]. It was already shown that transplantation of rat bone marrow MSCs [21] as well as human iPSC-derived hepatocytes [22] support liver regeneration and improve the disease phenotype in Gunn rats. In contrast to these studies, immunosuppression of host animals was omitted in our experiments and may explain the variations in engraftment observed in our study. Nevertheless, we could observe the therapeutic potential of human ESC- and iPSC-derived iMSCs for the treatment of liver diseases. Although bilirubin levels in Gunn rat blood serum were reduced in the transplanted groups in comparison to the control, serum bilirubin could not reach the values seen in wild-type rats. However, as previously described by others [31,32], we found evidence for a fusion of cells from human and rat origin. These fusion events may have led to a gene transfer from human to rat cells, thereby overcoming the host Ugt1a1 deficiency. With regard to this, cell fusion is apparently not negative per se. Indeed, cell fusion has been discussed as an option for therapeutic use [33,34]. However, we cannot exclude that human iMSCs differentiated into hepatocytes without fusion as described by others [9].

Despite transplanted human iMSCs acquiring hepatocyte functions, no shift from taurine- to glycine-conjugated bile acids was observed in the blood of Gunn rats, which could have mirrored the appearance of cells with properties of human hepatocytes in the rat liver [35]. However, an increased level of unconjugated bile acids was shown in the blood of Gunn rats after iMSC transplantation. Interestingly, in the rat, the blood concentration of unconjugated bile acids is substantially higher than the amount of conjugated bile acids [36]. The reason for elevated concentrations of unconjugated bile acids after iMSC transplantation is unclear.

Evidence for liver injury by the transplanted iMSCs was not observed, since the levels of AST, ALT, nor LDH were found to be elevated in the blood. Although there are publications describing MSC-mediated fibrosis [12] and fibrolysis-inhibiting human SERPINE1 was found in the blood of Gunn rats, we could not find any evidence for liver fibrosis in Gunn rats by histological examination and qPCR analysis of Collagen 1 and α-SMA. However, increased mRNA levels of Collagen 4, which is an essential element of the basement membrane-like structure in the space of Dissé of normal liver tissue, were observed in Gunn rats of the transplantation groups. Transplanted iMSCs could have released factors such as connective tissue growth factor that stimulated collagen expression in host liver tissue. Immunofluorescence analysis of liver sections exhibited neither elevated deposition of Collagen 4 nor scar formation. Thus, transplanted iMSCs contributed to liver regeneration of Gunn rats without obvious adverse effects. Since MSCs have been widely reported to release immunomodulatory factors [36–38], no immunosuppression was used in this study. Indeed, the transplanted human iMSCs survived within the Gunn rats for at least 2 months. However, long-term studies are necessary before use of iMSCs in clinical practice to ensure tumor safety for patients. Nevertheless, given their multipotentiality and immunomodulatory capacity, iMSCs seem to represent a valuable cell type for future autologous or allogeneic transplantations [14]. Our findings underpin the potential of iMSCs as an option for treating liver diseases and inherited liver disorders.

Acknowledgments

This study was supported by the German Research Foundation (DFG) through the Collaborative Research Center SFB 974 (''Communication and Systems Relevance during Liver Injury and Regeneration,'' Düsseldorf). Professor Dr. James Adjaye acknowledges support from the Federal Ministry of Education and Research-BMBF (01GN1005) and the Medical Faculty, Heinrich-Heine-University, Düsseldorf. Professor Dr. Richard Oreffo is supported by grants from the BBSRC (LO21072/1) and MRC (MR/K026682/1). The authors are grateful to Claudia Rupprecht (Clinic for Gastroenterology, Hepatology and Infectious Diseases) for expert technical assistance and Katharina Raba (Institute of Transplantation

Diagnostics and Cell Therapeutics) of the Heinrich Heine University for the FACS analyses. The authors acknowledge the Rat Resource & Research Center (P40OD011062) for providing Gunn rats.

Author Disclosure Statement

No competing financial interest exists.

References

1. Crigler JF Jr. and VA Najjar. (1952). Congenital familial nonhemolytic jaundice with kernicterus. Pediatrics 10:169–180.
2. Ruud Hansen TW. (2010). Phototherapy for neonatal jaundice—therapeutic effects on more than one level? Semin Perinatol 34:231–234.
3. Ramy N, EA Ghany, W Alsharany, A Nada, RK Darwish, WA Rabie and H Aly. (2016). Jaundice, phototherapy and DNA damage in full-term neonates. J Perinatol 36:132–136.
4. van Dijk R, U Beuers and PJ Bosma. (2015). Gene replacement therapy for genetic hepatocellular jaundice. Clin Rev Allergy Immunol 48:243–253.
5. Jorns C, G Nowak, A Nemeth, H Zemack, LM Mörk, H Johansson, R Gramignoli, M Watanabe, A Karadagi, et al. (2016). De novo donor-specific HLA antibody formation in two patients with Crigler–Najjar Syndrome Type I following human hepatocyte transplantation with partial hepatectomy preconditioning. Am J Transplant 16:1021–1030.
6. Gunn CK. (1944). Hereditary acholuric jaundice in the rat. Can Med Assoc J 50:230–237.
7. Dominici M, K Le Blanc, I Mueller, I Slaper-Cortenbach, F Marini, D Krause, R Deans, A Keating, Dj Prockop and E Horwitz. (2006). Minimal criteria for defining multipotent mesenchymal stromal cells. The International Society for Cellular Therapy position statement. Cytotherapy 8:315–317.
8. Crisan M, S Yap, L Casteilla, CW Chen, M Corselli, TS Park, G Andriolo, B Sun, B Zheng, et al. (2008). A perivascular origin for mesenchymal stem cells in multiple human organs. Cell Stem Cell 3:301–313.
9. Sato Y, H Araki, J Kato, K Nakamura, Y Kawano, M Kobune, T Sato, K Miyanishi, T Takayama, et al. (2005). Human mesenchymal stem cells xenografted directly to rat liver are differentiated into human hepatocytes without fusion. Blood 106:756–763.
10. Kuo TK, SP Hung, CH Chuang, CT Chen, YR Shih, SC Fang, VW Yang and OK Lee. (2008). Stem cell therapy for liver disease: parameters governing the success of using bone marrow mesenchymal stem cells. Gastroenterology 134:2111–2121, 2121.e1.
11. van Poll D, B Parekkadan, CH Cho, F Berthiaume, Y Nahmias, AW Tilles and ML Yarmush. (2008). Mesenchymal stem cell-derived molecules directly modulate hepatocellular death and regeneration in vitro and in vivo. Hepatology 47:1634–1643.
12. Kramann R, RK Schneider, DP DiRocco, F Machado, S Fleig, PA Bondzie, JM Henderson, BL Ebert and BD Humphreys. (2015). Perivascular Gli1+ progenitors are key contributors to injury-induced organ fibrosis. Cell Stem Cell 16:51–66.
13. Walker N, L Badri, S Wettlaufer, A Flint, U Sajjan, PH Krebsbach, VG Keshamouni, M Peters-Golden and VN Lama. (2011). Resident tissue-specific mesenchymal progenitor cells contribute to fibrogenesis in human lung allografts. Am J Pathol 178:2461–2469.
14. Jung Y, G Bauer and JA Nolta. (2012). Concise review: induced pluripotent stem cell-derived mesenchymal stem cells: progress toward safe clinical products. Stem Cells 30:42–47.
15. Frobel J, H Hemeda, M Lenz, G Abagnale, S Joussen, B Denecke, T Sarić, M Zenke and W Wagner. (2014). Epigenetic rejuvenation of mesenchymal stromal cells derived from induced pluripotent stem cells. Stem Cell Rep 3:414–422.
16. Wang X, EA Kimbrel, K Ijichi, D Paul, AS Lazorchak, J Chu, NA Kouris, GJ Yavanian, SJ Lu, et al. (2014). Human ESC-derived MSCs outperform bone marrow MSCs in the treatment of an EAE model of multiple sclerosis. Stem Cell Rep 3:115–130.
17. Hawkins KE, M Corcelli, K Dowding, AM Ranzoni, F Vlahova, KL Hau, A Hunjan, D Peebles, P Gressens, et al. (2018). Embryonic stem cell-derived mesenchymal stem cells (MSCs) have a superior neuroprotective capacity over fetal MSCs in the hypoxic-ischemic mouse brain. Stem Cells Transl Med 7:439–449.
18. Lian Q, Y Zhang, J Zhang, HK Zhang, X Wu, Y Zhang, FF Lam, S Kang, JC Xia, et al. (2010). Functional mesenchymal stem cells derived from human induced pluripotent stem cells attenuate limb ischemia in mice. Circulation 121: 1113–1123.
19. Gruenloh W, A Kambal, C Sondergaard, J McGee, C Nacey, S Kalomoiris, K Pepper, S Olson, F Fierro and JA Nolta. (2011). Characterization and in vivo testing of mesenchymal stem cells derived from human embryonic stem cells. Tissue Eng Part A 17:1517–1525.
20. Kimbrel EA, NA Kouris, GJ Yavanian, J Chu, Y Qin, A Chan, RP Singh, D McCurdy, L Gordon, RD Levinson and R Lanza. (2014). Mesenchymal stem cell population derived from human pluripotent stem cells displays potent immunomodulatory and therapeutic properties. Stem Cells Dev 23:1611–1624.
21. Muraca M, C Ferraresso, MT Vilei, A Granato, M Quarta, E Cozzi, M Rugge, KA Pauwelyn, M Caruso, et al. (2007). Liver repopulation with bone marrow derived cells improves the metabolic disorder in the Gunn rat. Gut 56:1725–1735.
22. Chen Y, Y Li, X Wang, W Zhang, V Sauer, CJ Chang, B Han, T Tchaikovskaya, Y Avsar, et al. (2015). Amelioration of hyperbilirubinemia in Gunn rats after transplantation of human induced pluripotent stem cell-derived hepatocytes. Stem Cell Rep 5:22–30.
23. Mirmalek-Sani SH, RS Tare, SM Morgan, HI Roach, DI Wilson, NA Hanley and RO Oreffo. (2006). Characterization and multipotentiality of human fetal femur-derived cells: implications for skeletal tissue regeneration. Stem Cells 24:1042–1053.
24. Megges M, RO Oreffo and J Adjaye. (2016). Episomal plasmid-based generation of induced pluripotent stem cells from fetal femur-derived human mesenchymal stromal cells. Stem Cell Res 16:128–132.
25. Chen YS, RA Pelekanos, RL Ellis, R Horne, EJ Wolvetang and NM Fisk. (2012). Small molecule mesengenic induction of human induced pluripotent stem cells to generate mesenchymal stem/stromal cells. Stem Cells Transl Med 1: 83–95.
26. Dirks WG and HG Drexler. (2013). STR DNA typing of human cell lines: detection of intra- and interspecies cross-contamination. Methods Mol Biol 946:27–38.
27. Higgins GM and RM Anderson. (1931). Experimental pathology of the liver. I. Restoration of the liver of the white rat following partial surgical removal. Arch Pathol Lab Med 12:186–202.

28. Herebian D and E Mayatepek. (2012). Analysis of bile acids by tandem mass spectrometry. In: *Hepatobiliary Transport in Health and Disease.* Häussinger D, V Keitel, R Kubitz, eds. Walter De Gruyter GmbH Co. KG, Berlin/Boston, pp 277–287.
29. Kordes C, I Sawitza, S Götze, D Herebian and D Häussinger. (2014). Hepatic stellate cells contribute to progenitor cells and liver regeneration. J Clin Invest 124:5503–5515.
30. O'Hagan-Wong K, S Nadeau, A Carrier-Leclerc, F Apablaza, R Hamdy, D Shum-Tim, F Rodier and I Colmegna. (2016). Increased IL-6 secretion by aged human mesenchymal stromal cells disrupts hematopoietic stem and progenitor cells' homeostasis. Oncotarget 7:13285–13296.
31. Vassilopoulos G, PR Wang and DW Russell. (2003). Transplanted bone marrow regenerates liver by cell fusion. Nature 422:901–904.
32. Wang X, H Willenbring, Y Akkari, Y Torimaru, M Foster, M Al-Dhalimy, E Lagasse, M Finegold, S Olson and M Grompe. (2003). Cell fusion is the principal source of bone marrow-derived hepatocytes. Nature 422:897–901.
33. Vassilopoulos G and DW Russell. (2003). Cell fusion: an alternative to stem cell plasticity and its therapeutic implications. Curr Opin Genet Dev 13:480–485.
34. Sullivan S and K Eggan. (2006). The potential of cell fusion for human therapy. Stem Cell Rev 2:341–349.
35. García-Cañaveras JC, MT Donato, JV Castell and A Lahoz. (2012). Targeted profiling of circulating and hepatic bile acids in human, mouse, and rat using a UPLC-MRM-MS-validated method. J Lipid Res 53:2231–2241.
36. Aggarwal S and MF Pittenger. (2005). Human mesenchymal stem cells modulate allogeneic immune cell responses. Blood 105:1815–1822.
37. Kaplan JM, ME Youd and TA Lodie. (2011). Immunomodulatory activity of mesenchymal stem cells. Curr Stem Cell Res Ther 6:297–316.
38. Trounson A and C McDonald. (2015). Stem cell therapies in clinical trials: progress and challenges. Cell Stem Cell 17:11–22.

Address correspondence to:
Prof. Dr. James Adjaye
Institute for Stem Cell Research and Regenerative Medicine
Heinrich Heine University, Düsseldorf
Moorenstraße 5
Düsseldorf 40225
Germany

E-mail: james.adjaye@med.uni-duesseldorf.de

Prof. Dr. Dieter Häussinger
Clinic of Gastroenterology, Hepatology and Infectious Diseases
Heinrich Heine University, Düsseldorf
Moorenstraße 5
Düsseldorf 40225
Germany

E-mail: haeussin@uni-duesseldorf.de

Received for publication January 15, 2018
Accepted after revision September 29, 2018
Prepublished on Liebert Instant Online September 29, 2018